

Organocatalytic, Enantioselective Intramolecular [6 + 2] Cycloaddition Reaction for the Formation of Tricyclopentanoids and Insight on Its Mechanism from a Computational Study

Yujiro Hayashi,^{*,†,§} Hiroaki Gotoh,[†] Masakazu Honma,[†] Kuppusamy Sankar,[†] Indresh Kumar,[†] Hayato Ishikawa,[†] Kohzo Konno,[‡] Hiroharu Yui,^{‡,§} Seiji Tsuzuki,^{||} and Tadafumi Uchimaru^{*,||}

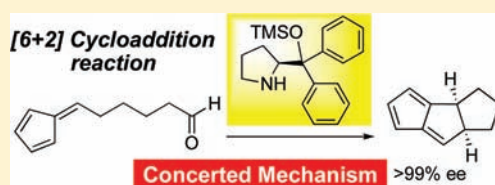
[†]Department of Industrial Chemistry, Faculty of Engineering, [‡]Department of Chemistry, Faculty of Science, and [§]Research Institute for Science and Technology, Tokyo University of Science, Kagurazaka, Shinjuku-ku, Tokyo 162-8601, Japan

^{||}Nanosystem Research Institute, National Institute of Advanced Industrial Science and Technology, Tsukuba, Ibaraki 305-8568, Japan

S Supporting Information

ABSTRACT: Diphenylprolinol silyl ether was found to be an effective organocatalyst for promoting the asymmetric, catalytic, intramolecular [6 + 2] cycloaddition reactions of fulvenes substituted at the exocyclic 6-position with a δ -formylalkyl group to afford synthetically useful linear triquinane derivatives in good yields and excellent enantioselectivities. The *cis*-fused triquinane derivatives were obtained exclusively; the *trans*-fused isomers were not detected among the reaction products. The intramolecular [6 + 2] cycloaddition occurs

between the fulvene functionality (6π) and the enamine double bond (2π) generated from the formyl group in the substrates and the diphenylprolinol silyl ether. The absolute configuration of the reaction products was determined by vibrational circular dichroism. The reaction mechanism was investigated using molecular orbital calculations, B3LYP and MP2 geometry optimizations, and subsequent single-point energy evaluations on model reaction sequences. These calculations revealed the following: (i) The intermolecular [6 + 2] cycloaddition of a fulvene and an enamine double bond proceeds in a stepwise mechanism via a zwitterionic intermediate. (ii) On the other hand, the intramolecular [6 + 2] cycloaddition leading to the *cis*-fused triquinane skeleton proceeds in a concerted mechanism via a highly asynchronous transition state. (iii) The fulvene functionality and the enamine double bond adopt the *gauche-syn* conformation during the C–C bond formation processes in the [6 + 2] cycloaddition. (iv) The energy profiles calculated for the intramolecular reaction explain the observed exclusive formation of the *cis*-fused triquinane derivatives in the [6 + 2] cycloaddition reactions. The reasons for the enantioselectivity seen in these [6 + 2] cycloaddition reactions are also discussed.



INTRODUCTION

Cycloaddition reactions are one of the most powerful methods for the construction of cyclic skeletons.¹ However, as compared to the well-established [4 + 2] cycloaddition (Diels–Alder) reaction,² only a few [6 + 2] cycloaddition reactions are known. In fact, concerted [6 + 2] cycloaddition reactions are forbidden by the Woodward–Hoffmann rules when the reaction is thermally activated and the two reacting π systems add in a suprafacial fashion.³ On the other hand, transition metals can promote the [6 + 2] cycloaddition reactions of 1,3,5-cycloheptatriene,⁴ and the intramolecular [6 + 2] cycloaddition of vinylcyclobutanones.⁵ Fulvene moieties are known to act as the 6π -component in some [6 + 2] cycloaddition reactions, and Hong has reported an intermolecular [6 + 2] cycloaddition reaction of aminofulvenes with electron-deficient alkenes,⁶ while Houk disclosed an intramolecular [6 + 2] cycloaddition reaction of fulvene with enamines⁷ to afford linearly fused tricyclopentanoids. As far as we are aware, there is only one report of an enantioselective [6 + 2] cycloaddition reaction, that between cycloheptatriene and alkynes catalyzed by a chiral cobalt reagent.^{4e,8}

One theme in the rapidly developing field of organocatalysts⁹ has been their successful application to cycloaddition reactions such as the [4 + 2] cycloaddition reaction,¹⁰ [3 + 2] cycloaddition reaction,¹¹ [2 + 2] cycloaddition reaction,¹² [4 + 3] cycloaddition reaction,¹³ and [2 + 1] cycloaddition reaction.¹⁴ Diarylprolinol silyl ether,¹⁵ which has been developed independently by our group¹⁶ and Jørgensen's group,¹⁷ is an effective organocatalyst, which has been employed in several asymmetric reactions. We have also developed diarylprolinol silyl ether-mediated cycloadditions such as the Diels–Alder reaction,^{16e,h} formal aza [3 + 3] cycloaddition reaction,^{16f} and formal carbo [3 + 3] cycloaddition reaction.^{16j} Our interest in the application of diphenylprolinol silyl ether to cycloaddition reactions promoted us to investigate its use in the intramolecular formal [6 + 2] cycloaddition reaction of fulvenes, which will be described in this Article.

RESULTS AND DISCUSSION

Houk has already reported that fulvenes substituted at the exocyclic 6-position by a 6-(ω -formylalkyl)group react with an

Received: January 10, 2010

Published: November 03, 2011

equimolar amount of Et_2NH and K_2CO_3 in the presence of molecular sieves in benzene to afford tricyclopentanoids by the successive reactions of enamine generation, $[6 + 2]$ cycloaddition, and deamination.⁷ As there is no asymmetric version of this reaction, and the cyclopentanoids obtained are useful chiral intermediates that form the key framework of several natural products, we started to investigate this reaction using chiral organocatalysts (see Figure 1). We selected 4,4-bis(methoxycarbonyl)-6-(2,4-cyclopentadien-1-ylidene)hexanal **3a** as a model substrate, which was easily synthesized from dimethyl malonate as shown in Scheme 1. Dimethyl malonate was successively alkylated with (*p*-methoxyphenyl)methoxypropyl iodide and allyl bromide. Oxidative cleavage of the allyl double bond with a catalytic amount of OsO_4 and NaIO_4 gave an aldehyde, which was treated with cyclopentadiene to provide a fulvene derivative. After removal of the PMB protecting group with DDQ, oxidation of the resulting alcohol proceeded smoothly to afford **3a** in good yield.

The intramolecular $[6 + 2]$ cycloaddition reaction of **3a** was examined in detail (see eq 1) with the results summarized in Table 1. When proline was used as catalyst in toluene, the desired triquinane **4a** was obtained in 15% yield with low ee (39% ee, entry 1). The enantioselectivity dramatically increased to 98% when a catalytic amount of diphenylprolinol silyl ether **1** was employed (10 mol %), albeit the product yield was low (entry 2). To increase the yield, additives were investigated. Whereas NaOAc was not suitable (entry 3), benzoic acid was found to be effective, affording the product **4a** in good yield (89%) and excellent enantiomeric purity (98% ee, entry 4). Screening of solvents indicated that toluene was the optimal choice (entries 4–9). It should be noted that trifluoromethyl-substituted diarylprolinol silyl ether **2** was not effective in the present reaction (entry 10).

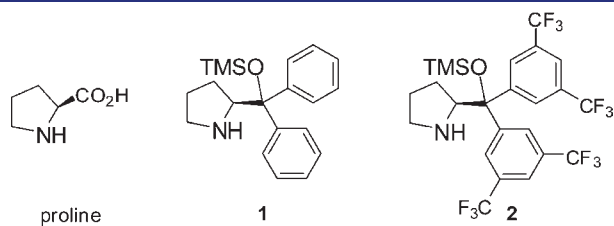
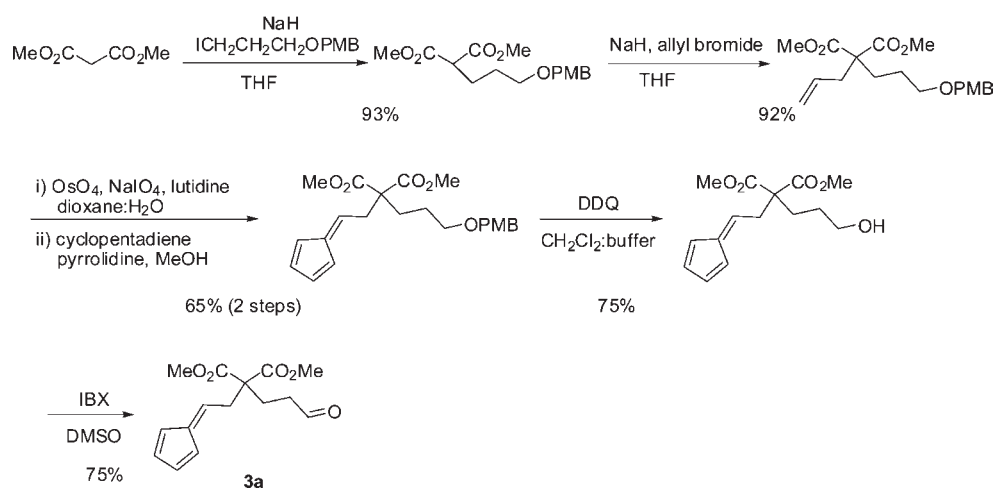


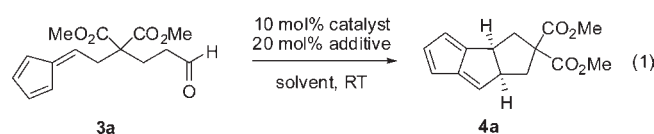
Figure 1. Organocatalysts examined in this study.

Scheme 1. Synthesis of **3a**



As excellent results had been obtained for the model compound **3a**, the generality of the reaction was examined (Table 2). The reaction proceeds efficiently without any substituent on the tether as in 6-(2,4-cyclopentadien-1-ylidene)hexanal **3b**, which gives the triquinane **4b** of excellent enantiomeric purity (entry 2). It should be noted that the reaction catalyzed by 10 mol % of diphenylprolinol silyl ether **1** in the presence of PhCO_2H is fast and is complete within 3 h for the formation of **4b**, while it is reported that it takes 24 h to go to completion in the presence of an equimolar amount of Et_2NH , K_2CO_3 , and molecular sieves in benzene.⁷ Nearly optically pure **4c**, a useful synthetic intermediate, was formed in good yield from the substrate **3c** possessing a dithiane moiety (entry 3). Linear tetracycles **4d**, **4e**, **4f**, and **4g** were also synthesized in excellent enantiomeric purity (entries 4–7). It is worth noting that indoline derivative **4e**, which is also a useful chiral intermediate, was prepared from the acyclic aniline precursor **3e** via this $[6 + 2]$ cycloaddition reaction (entry 5).

Table 1. Effect of the Catalyst and Solvent on the $[6 + 2]$ Cycloaddition Reaction of **3a**^a



entry	cat.	additive	solvent	time (h)	yield (%) ^b	ee (%) ^c
1	proline		toluene	6	15	39
2	1		toluene	3	21	98
3	1	NaOAc	toluene	3	39	96
4	1	PhCO_2H	toluene	3	89	98
5	1	PhCO_2H	benzene	1.5	65	99
6	1	PhCO_2H	CH_2Cl_2	0.5	60	96
7	1	PhCO_2H	MeCN	0.5	68	97
8	1	PhCO_2H	DMF	3	63	92
9	1	PhCO_2H	MeOH	3	39	98
10	2	PhCO_2H	toluene	25	<5	

^a Reaction conditions: aldehyde **3a** (0.3 mmol), catalyst (0.03 mmol), and additive (0.06 mmol) in solvent (3.0 mL) at room temperature for the indicated time. ^b Isolated yield. ^c The ee's are determined on chiral stationary phase HPLC.

Table 2. Catalytic Asymmetric [6 + 2] Cycloaddition Reaction with Various Substrates^a

Reaction scheme showing the catalytic asymmetric [6 + 2] cycloaddition of a substituted fulvene (3) with an aldehyde (R-CHO) to form a triquinane derivative (4). Conditions: 10 mol% **1**, 20 mol% PhCO₂H, toluene, RT.

Entry	Starting material	Product	Time (h)	Yield (%) ^b	Ee (%) ^c
1			3	89	98
2			3	61	>99
3			3	85	>99
4			6	79	96
5			2.5	83	98
6 ^d			36	52	82
7 ^d			36	61	90
8			36	57	90
9			5	77	98
10			6	70	96
11 ^e			24	25	nd ^f

^a Reaction conditions: Aldehyde **3** (0.3 mmol), catalyst **1** (0.03 mmol), and PhCO₂H (0.06 mmol) in toluene (3.0 mL) at room temperature for the indicated time. ^b Isolated yield. ^c The ee's are determined by chiral stationary phase HPLC or GC. ^d Reaction temperature is -40°C . ^e Catalyst (20 mol %) was employed. ^f nd = not determined.

Dihydrobenzofuran derivatives **4f** and **4g** were also prepared efficiently from the acyclic phenol precursors **3f**, **3g** (entries 6, 7).

p-Bromo-substituted phenol derivative **3g** is a suitable precursor for the [6 + 2] cycloaddition reaction, affording the product **4g** in 90% ee (entry 7). Further transformations of this compound, including cross-coupling reactions, would be possible because of the arylbromo functional group. Oxa-analogue **4h** was also synthesized from the α -alkoxyaldehyde **3h** in excellent enantiomeric purity (entry 8). Thus, NCbz and ether functional groups do not interfere with the reaction, and both chiral aza- and oxa-analogues can be obtained in excellent enantiomeric purity. Not only 6-monosubstituted fulvene derivatives, but also 6,6-disubstituted fulvenes such as **3i** are suitable substrates, affording the triquinane derivative **4i** possessing a quaternary chiral center in excellent enantiomeric purity (entry 9). Up to this point, only the synthesis of the triquinane ring system by the formation of two new five-membered rings had been examined. Next, concomitant formation of a five- with a six-membered ring was investigated using **3j** having a naphthalene moiety in the tether chain. This reaction proceeds smoothly and with high enantioselectivity to afford the cyclized product **4j** in good yield (entry 10). Contrary to the successful result of entry 10, the reaction of **3k** that contains bismethoxycarbonyl substituents on the tether chain was very slow, and starting material was recovered even though the catalyst **1** was employed in 20 mol % (entry 11). Thus, the triquinane ring system can be easily prepared by this asymmetric double five-membered ring closure, while 5 + 6-membered ring formation can proceed when the reacting formyl group and fulvene unit are held in close proximity.

Determination of the Absolute Configuration. The absolute configuration of **4d** was determined by vibrational circular dichroism (VCD). Calculations of IR and VCD spectra for **4d** were carried out using Gaussian 03.¹⁸ The geometry of **4d** was optimized by using density functional theory (DFT), which was performed with B3LYP functional and the 6-311G+(2d,p) basis set. The pattern and sign of the calculated VCD spectrum agreed well with those of the experimental VCD spectrum in the region of 1700–1200 cm⁻¹ (Figure 2). For example, experimental VCD bands at 1481, 1473, and 1458 cm⁻¹ showed a (+, -, +) pattern. This pattern was reproduced by the calculated VCD bands at 1480, 1471, and 1455 cm⁻¹.

Theoretical Study. *Postulated Reaction Mechanism and Calculation Model.* According to the reaction mechanism proposed by Houk for the racemic intramolecular [6 + 2] cycloaddition reaction,⁷ the following sequence would be postulated for the conversion of the substrate **3** to the triquinane derivative **4** (Figure 3): (i) the formyl group in **3** reacts with the amine catalyst **1** to generate the corresponding enamine **5**, (ii) the enamine double bond and the fulvene functionality undergo intramolecular [6 + 2] cycloaddition via zwitterion **5'** (vide infra), and then (iii) the amine catalyst **1** is expelled from the addition product to afford the triquinane derivative **4**. There are two possible reaction paths from **5'** to product. One is the attack of cyclopentadienyl anion on iminium ion, followed by the elimination of amine catalyst **1** generating the addition product (path A). The other is the hydrolysis of iminium ion **5'** by water with the release of catalyst, followed by an intramolecular addition reaction and dehydration to provide the addition product (path B). If the reaction proceeds via pathway B, it will fail under anhydrous conditions as hydrolysis of the iminium ion cannot occur. When performed under anhydrous conditions in the presence of molecular sieves using compound **3h**, which is not a reactive substrate, requiring 36 h for completion of the reaction under standard conditions, the reaction proceeded equally as well,

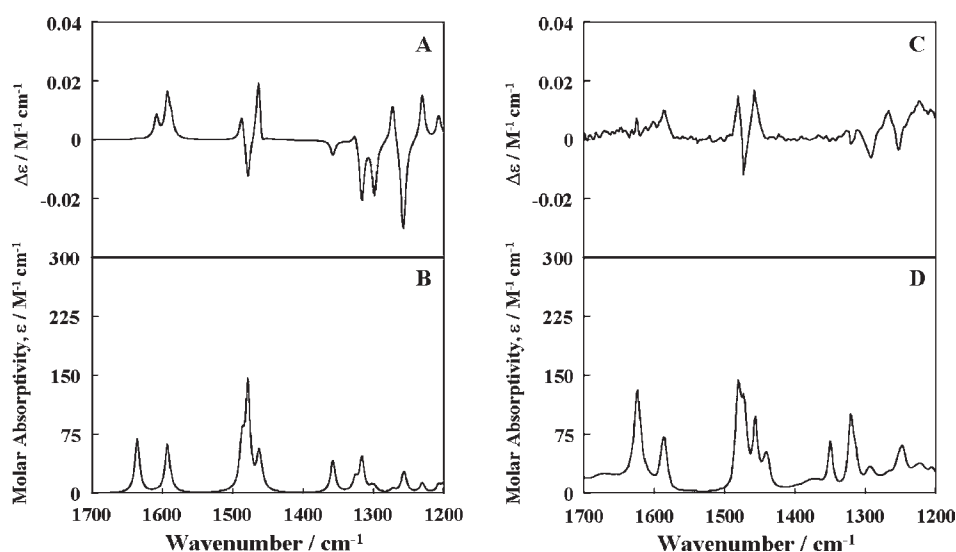


Figure 2. Top: Comparison of calculated (A) and experimental VCD spectra (C) of **4d**. Bottom: Comparison of calculated (B) and experimental IR spectra (D) of **4d**.

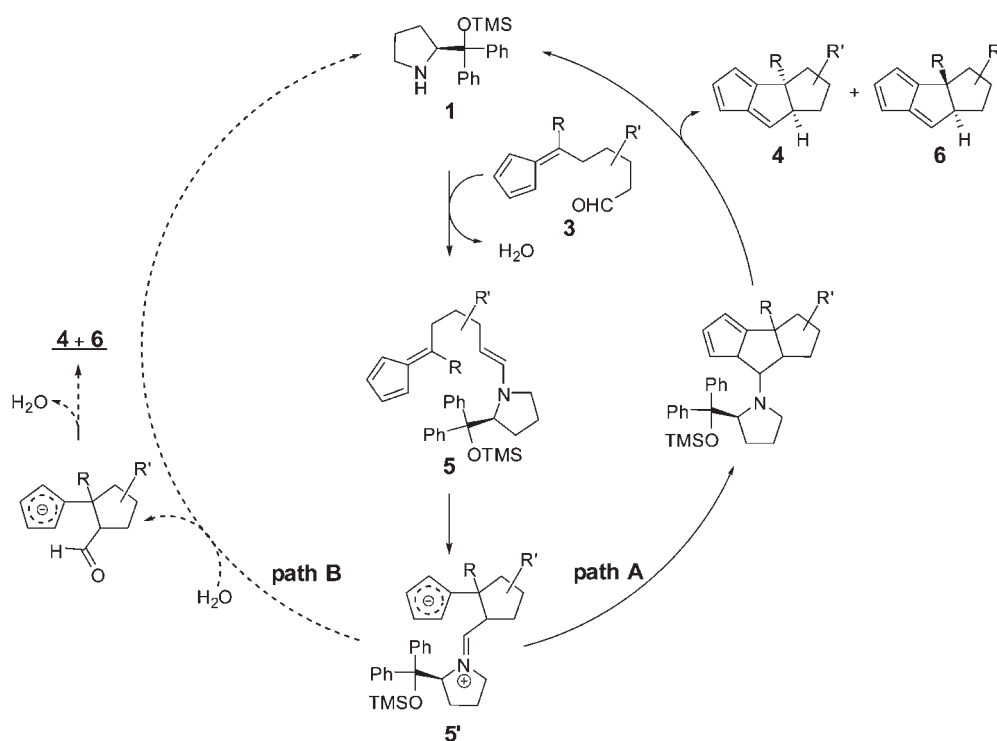


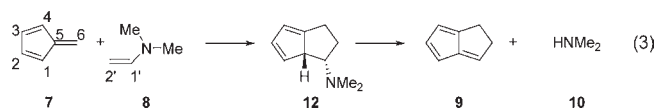
Figure 3. Mechanism postulated for the intramolecular [6 + 2] cycloaddition reaction. The *cis*-fused triquinane derivatives **4** are formed exclusively. The *trans*-fused isomers **6** were not detected among the reaction products.

and there was no effect of molecular sieves on either reactivity or enantioselectivity. Therefore, the reaction proceeds via direct attack of the cyclopentadienyl anion on the iminium ion (path A).

To model the [6 + 2] cycloaddition reaction of **5**, we investigated the intermolecular reaction of fulvene **7** and enamine (*N,N*-dimethylvinylamine) **8** (eq 3). Two C–C bonds are formed in this reaction. One is that between the double bond terminal (the 2'-position) of enamine **8** and the exocyclic

6-position of fulvene **7**. The other is that between the nitrogen neighboring position (the 1'-position) of enamine **8** and the 1-position (or the 4-position) of fulvene **7**. Elimination of dimethylamine **10** from the cycloaddition product **12** yields bicyclic compound **9**. The reaction sequence given in eq 3 corresponds to the conversion of the enamine intermediate **5** to the triquinane derivative **4** with the regeneration of the catalyst **1**. We also carried out calculations on the intramolecular [6 + 2] cycloaddition reaction of **5a** ($R = R' = H$, $NR''_2 =$

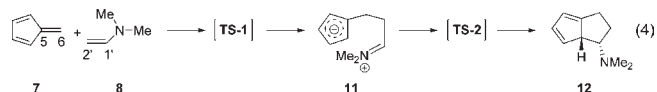
NMe₂, Figure 3; see also Figure 8). To the best of our knowledge, this is the first systematic theoretical study on the mechanism of a [6 + 2] cycloaddition reaction.



Computational Methodology. The Gaussian 03 program¹⁸ was used for the molecular orbital calculations. Geometry optimizations were performed at the hybrid density functional theory (B3LYP)¹⁹ and the MP2²⁰ levels using the 6-311G(d,p) basis set.²¹ Frequency calculations were carried out for the optimized structures to verify the stationary points as energy minima or saddle points. In addition, by using the intrinsic reaction coordinate (IRC) procedure, we followed minimum energy paths from the transition states to verify the nature of the reactants and products.²²

Single-point energies of the optimized stationary points for the model reaction eq 3 were computed with the MP2 method and coupled cluster calculations with single and double substitutions with noninteracting triple excitations [CCSD(T)].²³ We calculated CCSD(T) level relative energy at the basis set limit [$E_{\text{CCSD(T)}(\text{limit})}$] of each stationary point (the energy difference between each stationary point and the reactants 7 and 8).²⁴ Solvation corrections for the experimentally used solvent, toluene, were calculated by using the CPCM method²⁶ and the UAKS radii with single-point HF/6-31+G(d) level of theory²⁷ at the MP2-optimized geometries.

[6 + 2] Cycloaddition Reaction of 7 and 8. For the [6 + 2] cycloaddition reaction of fulvene 7 and enamine 8 (eq 3), the B3LYP and MP2 levels of calculations both suggested a stepwise C–C bond formation mechanism via an intermediate. First, a C–C bond is formed between the 2'-position of enamine 8 and the exocyclic 6-position of fulvene 7 to yield the intermediate 11. Next, ring-closure of the intermediate 11 forming the second C–C bond results in the cycloaddition product 12 (eq 4). Population analysis indicates that the intermediate 11 has zwitterionic character. The dimethylamino group and the fulvene moiety in 11 are positively and negatively charged, respectively.²⁸ Therefore, formation of the intermediate 11 can be considered as arising from nucleophilic attack of the enamine moiety at the exocyclic 6-position of fulvene, resulting in an anionic cyclopentadiene ring and formation of an iminium ion. Transition states TS-1 and TS-2 were located for the first and the second C–C bond formation steps, respectively.²⁹ Neither B3LYP level calculations nor MP2 level calculations located a pathway for a concerted mechanism; that is, simultaneous formation of the two C–C bonds is unlikely for 7 and 8.



Optimized structures of the zwitterionic intermediate 11, the transition states TS-1 and TS-2, and the cycloaddition product 12 are shown in Figure 4. Three models can be postulated for how the enamine double bond approaches the fulvene functionality in the [6 + 2] cycloaddition reaction, *gauche-syn* (A), *gauche-anti* (B), and *antiperiplanar* (C) (Figure 5). The B3LYP and MP2 transition states differ somewhat in the forming bond lengths (Table 3), but both calculations suggest that fulvene 7 and

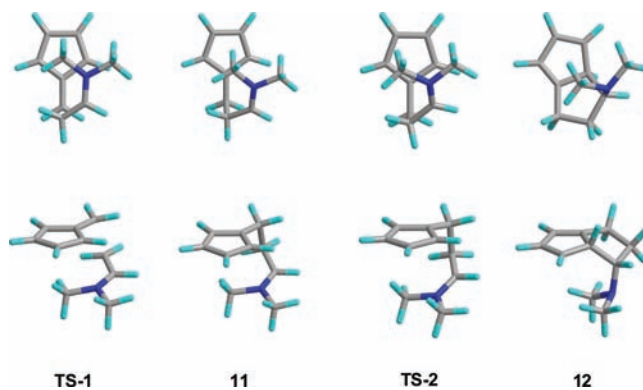


Figure 4. Top and side views of the structures of the zwitterionic intermediate 11, the transition states TS-1 and TS-2, and the cycloaddition product 12.

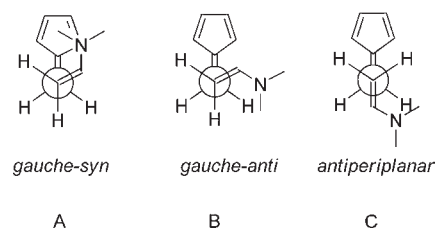


Figure 5. Possible approaches of the enamine double bond toward the fulvene functionality: (A) *gauche-syn*, (B) *gauche-anti*, and (C) *antiperiplanar*.

enamine 8 approach each other in the *gauche-syn* configuration (Figure 5 A). The dihedral angle of C5–C6–C2'–C1' (see eq 3 and 4 for atom numbering) is around -60° in TS-1, and the value of this dihedral angle remains almost unchanged in the zwitterionic intermediate 11 and TS-2 (Table 3). We tried to locate energy minima for the *gauche-anti* (B) and *antiperiplanar* (C) conformers (Figure 5) of the intermediate through rotation of the C6–C2' single bond in the zwitterionic intermediate 11, but such potential energy minima were not found.³⁰ The *gauche-syn* conformation in TS-2 would result in a *trans* relationship between the dimethylamino group and the bridgehead hydrogen atom in the cycloaddition product 12.³¹

The gas-phase and solution-phase relative enthalpy values of the stationary points in eq 4, as well as their CCSD(T) level relative electronic energies at the basis set limit ($E_{\text{CCSD(T)}(\text{limit})}$), are given in Table 4. Relative enthalpy values are schematically plotted in Figure 6. The gas-phase enthalpy values at 298 K indicate that the zwitterionic intermediate 11 and the two transition states for the [6 + 2] cycloaddition process TS-1 and TS-2 are higher in energy than the reactants fulvene 7 and enamine 8 by 7.03, 9.48, and 9.90 kcal/mol, respectively. The gas-phase enthalpy values of the cycloaddition product 12 and the final products (9 + 10) are lower than that of the reactants by 22.38 and 12.67 kcal/mol, respectively.³²

Intramolecular [6 + 2] Cycloaddition Reaction of Enamine 5. Seebach et al. have systematically investigated the X-ray crystal structures and NMRs of enamines derived from diarylprolinol ethers and aldehydes. Preferences for the C–N single bond to adopt the *s-trans* conformation and for the enamine double bond to adopt the *E* configuration have been pointed out (Figure 7).³³

Table 3. Calculated Values for the Energies and Geometric Parameters of the Zwitterionic Intermediate 11 and the Transition States TS-1 and TS-2

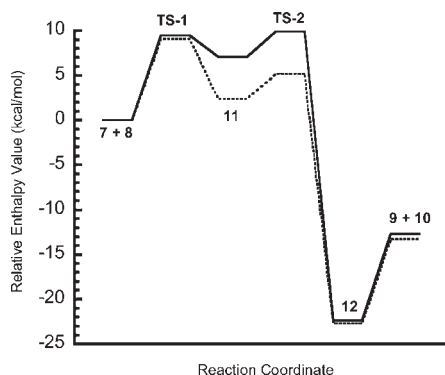
	11		TS-1		TS-2	
	B3LYP ^a	MP2 ^b	B3LYP ^a	MP2 ^b	B3LYP ^a	MP2 ^b
energy (au)	-444.857229	-443.472935	-444.854871	-443.466225	-444.849224	-443.467170
imaginary freq			348.5	256.4	263.7	152.0
geometric parameter (in Å and deg) ^c						
C5–C6	1.4611	1.4701	1.4131	1.3899	1.4918	1.4951
C6–C2'	1.6714	1.6298	1.9493	2.1667	1.5741	1.5705
C1'–C2'	1.4452	1.4526	1.4012	1.3832	1.4809	1.4793
C2'–N	1.3154	1.3076	1.3327	1.3456	1.3080	1.2923
C1–C1'	3.4229	3.2171	3.5173	3.3607	2.8962	2.8612
C5–C6–C2'	113.59	112.26	112.37	108.78	109.25	108.82
C6–C2'–C1'	108.94	105.34	105.89	98.25	109.78	104.62
C2'–C1'–N	125.63	124.21	126.80	125.95	128.10	128.12
C1–C5–C6–C2'	91.59	89.82	90.81	89.19	74.23	84.24
C4–C5–C6–C2'	-77.92	-80.25	-80.85	-87.60	-87.66	-76.38
C5–C6–C2'–C1'	-62.80	-59.76	-61.11	-55.43	-53.59	-48.31

^aOptimized at the B3LYP/6-311G(d,p) level. ^bOptimized at the MP2/6-311G(d,p) level. ^cSee eq 3 for atom numbering.

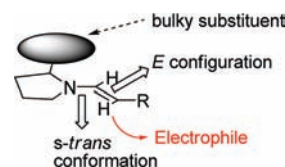
Table 4. CCSD(T) Relative Energies at the Basis Set Limit and Gas-Phase and Solution-Phase Enthalpy Values of the Stationary Points^a

	$E_{\text{CCSD(T)}(\text{limit})}^b$	$H(0\text{ K})^c$	$H(298\text{ K})^d$	$H(298\text{ K}) + E_{\text{sol}}^e$
7 + 8	0.00	0.00	0.00	0.00
TS-1	8.43	10.00	9.48	9.05
11	4.54	7.77	7.03	2.40
TS-2	7.72	10.70	9.90	5.21
12	-26.25	-21.20	-22.38	-22.68
9 + 10	-14.51	-12.41	-12.67	-13.29

^aEnergy values are given in kcal/mol. ^bCCSD(T) relative energies at the basis set limit. See the Supporting Information. ^cGas-phase relative enthalpy value at 0 K. ^dGas-phase relative enthalpy value at 298 K. ^eRelative enthalpy value at 298 K including solvation energy.

**Figure 6.** Schematically plotted gas-phase (—) and solution-phase (---) relative enthalpy values (at 298 K) for the stationary points. Numerical values are given in Table 4.

Considering these conformational preferences in the enamine moiety, two *gauche-syn* transition structures can be postulated for the first C–C bond formation step in 5 (Figure 8). The struc-

**Figure 7.** Preferable conformation and reaction pattern of the enamines derived from diarylprolinol ethers.

tures D and E will yield the *cis*- and *trans*-zwitterionic intermediates 13 and 14, respectively. We have been unable to detect either of these by NMR. For the *cis* intermediate 13, intramolecular [6 + 2] cycloaddition affords the *cis*-fused tricyclic adduct 15. As seen in the stereochemistry of cycloaddition product 12, the *gauche-syn* approach will produce the *trans* relationship between the pyrrolidine ring and the bridgehead hydrogen atom in 15. The experimental conditions are weakly acidic, and prolinol silyl ether catalyst (HNR''₂) will thus be rapidly eliminated in an *antiperiplanar* manner from 15 to give the *cis*-fused triquinane skeleton 4. Were the same reaction sequence to occur, the *trans*-zwitterionic intermediate 14 would be converted to the *trans*-fused triquinane skeleton 6 via the *trans*-fused tricyclic adduct 16 (Figure 8). Protonation of 13 and 14 might occur to afford cyclopentadiene intermediates 13' and 14', which could revert again to 13 and 14 by deprotonation because cyclopentadiene is acidic. The direct transformation of 13' and 14' to starting material 5 by base-mediated elimination as shown in Figure 9 might also be possible.

The experiments indicate, however, that the *trans*-fused triquinane derivatives 6 are not produced. The *cis*-fused derivatives 4 were obtained exclusively. Houk et al. pointed out the possibility of reversible formation of the *cis*- and *trans*-zwitterionic intermediates, and that only *cis* intermediates will cyclize, giving the *cis*-fused triquinane skeleton, because the *trans*-fused isomer is considerably more ring strained than the *cis* (Figure 8).⁷ There are two seemingly plausible reaction paths for the isomerization between 13 and 14. One is retro reaction via starting material 5

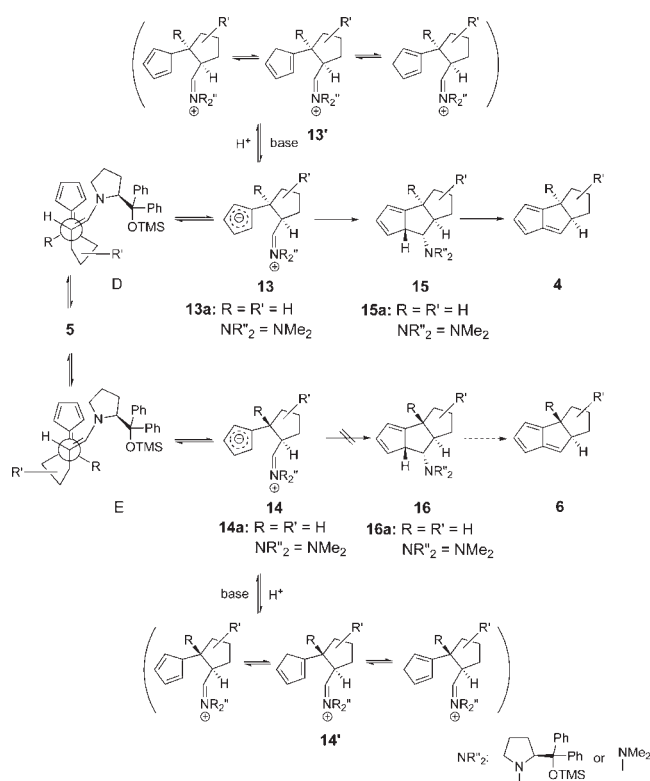


Figure 8. Postulated reaction paths for the conversion of enamine **5** into the triquinane skeleton.

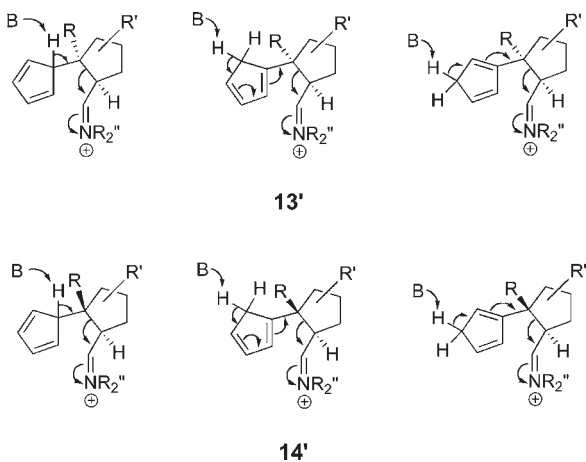


Figure 9. Postulated mechanism for conversion of protonated intermediates **13'** and **14'** to starting material **5**.

($13 \rightleftharpoons 5 \rightleftharpoons 14$). The other is the direct isomerization of **13** and **14** ($13 \rightleftharpoons 14$) via enamine–iminium tautomerization. However, in the latter path, overall enantioselectivity would erode because inversion of the labile stereocenter of **14** would lead to ent-**13**. As high enantioselectivity is realized, the former must be the actual path taken. We carried out calculations on the simplest models of the *cis*- and *trans*-fused adducts, **15a** and **16a** ($R = R' = H, NR''_2 = NMe_2$, Figure 8). B3LYP and MP2 calculations using the 6-311G(d,p) basis set make the *trans*-fused isomer **16a**, respectively, 9.65 and 11.70 kcal/mol higher in energy than the *cis*-fused adduct **15a** (see Figure 12, including the zero-point energies³⁴). Meanwhile,

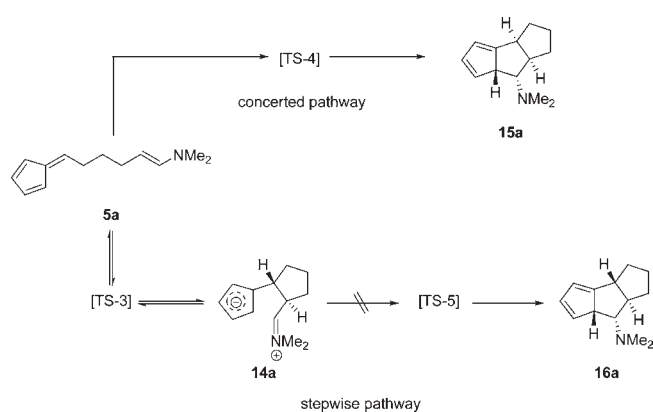


Figure 10. Pathways suggested for intramolecular [6 + 2] cycloaddition of **5a** in the present work.

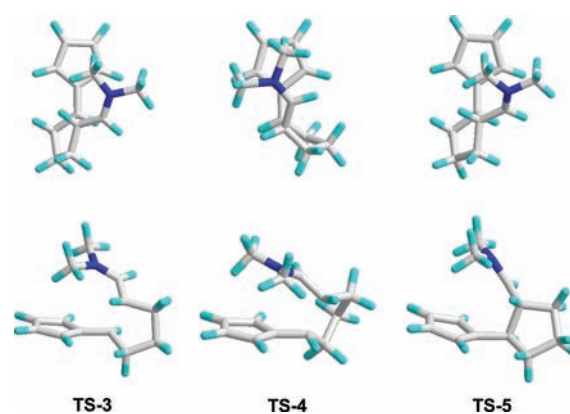


Figure 11. Top and side views of the structures of **TS-3**, **TS-4**, and **TS-5**.

B3LYP and MP2 calculations of the *cis*- and *trans*-zwitterionic intermediates **13a** and **14a** indicate that both isomers take the *gauche-syn* conformation, and that the *trans*-isomer **14a** is slightly lower in energy than the *cis* isomer **13a**.³⁵

In addition, we located the transition states **TS-4** and **TS-5** leading to the *cis*- and *trans*-fused adducts **15a** and **16a**, respectively. Surprisingly, the IRC calculation indicates that **TS-4** connects directly **5a** and the *cis*-fused tricyclic isomer **15a**. We were not able to locate a transition state connecting the putative *cis*-zwitterionic intermediate **13a** and *cis*-fused product **15a**. Meanwhile, **TS-5** connects the *trans*-zwitterionic intermediate **14a** and the *trans*-fused tricyclic product **16a**. **TS-3** was located separately for the formation of the *trans*-zwitterionic intermediate **14a** (Figure 10). These results indicate a concerted pathway via **TS-4** for the conversion of **5a** to the *cis*-fused tricyclic skeleton **15a**. The zwitterionic intermediate **13a** does not exist along the reaction coordinate for the [6 + 2] cyclization. On the other hand, a stepwise mechanism via **TS-3**, the zwitterionic intermediate **14a**, and **TS-5** is suggested for the conversion of **5a** to the *trans*-fused tricyclic isomer **16a** (Figure 10). The structures of **TS-3**–**TS-5** are given in Figure 11. The fulvene and enamine functionalities adopt the *gauche-syn* configuration in these transition states as well.

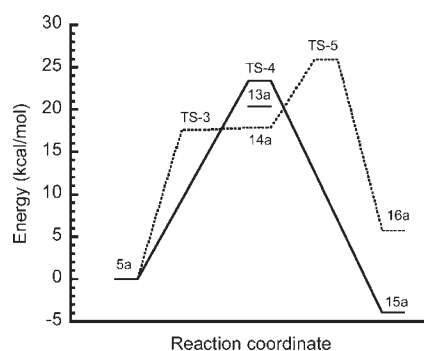
The B3LYP and MP2-optimized forming bond (C6–C2') lengths in **TS-3** are 1.7984 and 2.1236 Å, respectively. The corresponding forming bond (C1–C1') lengths in **TS-5** are

Table 5. Calculated Values for the Energies and the Bond Distances of the Zwitterionic Intermediates 13a and 14a, the Tricyclic Intermediates 15a and 16a, and Transition States TS-3–TS-5^a

	13a		14a		15a		16a	
	B3LYP ^b	MP2 ^c	B3LYP	MP2	B3LYP	MP2	B3LYP	MP2
energy	-561.614061	-559.874746	-561.617602	-559.876667	-561.655573	-559.926433	-561.640005	-559.907372
C6–C2' ^d	1.7468	1.6755	1.7578	1.6701	1.5822	1.5731	1.5487	1.5431
C1–C1' ^e	3.3688	3.1873	3.5339	3.3123	1.5751	1.5404	1.5880	1.5749

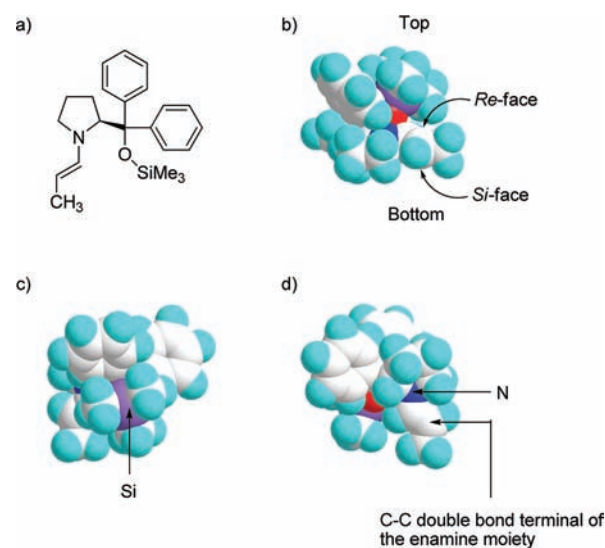
	TS-3		TS-4		TS-5	
	B3LYP	MP2	B3LYP	MP2	B3LYP	MP2
energy	-561.617599	-559.874138	-561.608444	-559.870072	-561.604882	-559.865051
imaginary freq	130.4	192.3	177.3	275.3	185.9	89.4
C6–C2' ^d	1.7984	2.1236	1.7200	1.8180	1.5664	1.5274
C1–C1' ^e	3.5472	3.4697	3.0939	3.1557	2.8310	2.4960

^aEnergies, imaginary frequencies, and bond distances are given in au, cm⁻¹, and Å, respectively. ^bB3LYP/6-311G(d,p) optimized results. ^cMP2/6-311G(d,p) optimized results. ^dBond distance between the 6-position of the fulvene moiety and the C–C double bond terminus of the enamine moiety. ^eBond distance between the 1-position of the fulvene moiety and the carbon atom adjacent to the nitrogen of the enamine moiety.

**Figure 12.** B3LYP/6-311G(d,p) calculated energies (including the zero-point energies³⁴) relative to the IRC end point of 5a are plotted.³⁷

2.8310 and 2.4960 Å (Table 5). These two C–C bonds will be formed simultaneously in the concerted transition state TS-4. However, TS-4 shows highly asynchronous character: C–C bond formation at the 1-position of the fulvene moiety (C1–C1') proceeds significantly behind C–C bond formation at the 6-position of the fulvene moiety (C6–C2') (see Table 5).³⁶ Although the two bonds are being formed concertedly in TS-4, the forming bond lengths indicate that TS-4 can be characterized as an almost pure transition state for nucleophilic attack by the enamine moiety at the 6-position of the fulvene functionality.

Energy profiles for the reaction paths from 5a to the *cis*- and *trans*-fused adduct 15a and 16a are given in Figure 12. For stepwise formation of the *trans*-fused isomer 16a (Figure 10), the second cyclization step via TS-5 is rate-limiting. TS-5 for the second cyclization step is higher in energy by 8.35 and 6.80 kcal/mol (including the zero-point energies³⁴) than TS-3 for the first cyclization step in B3LYP and MP2 calculations, respectively. Meanwhile, B3LYP and MP2 calculations, respectively, suggest that the highly asynchronous TS-4, leading concertedly to the *cis*-fused tricyclic isomer (Figure 10), is lower in energy by 2.58 and 3.85 kcal/mol than the rate-limiting TS-5 for stepwise formation of the *trans*-fused counterpart.³⁸ These results indicate that the

**Figure 13.** (a) Chemical structure of the model enamine prepared from propanal and diphenylprolinol silyl ether 1; (b) side view of the model enamine; (c) top view of the model enamine, and (d) bottom view of the model enamine. The *Re* face of the C–C bond terminal of the enamine moiety is effectively blocked by the diphenyltrimethylsilyloxymethyl group.

concerted formation of the *cis*-fused tricyclic product 15a via TS4 will be energetically favored over stepwise formation of the *trans*-fused counterpart 16a.

Exclusive formation of the *cis*-fused triquinane skeleton can be rationalized as the result of reversible formation of the *trans*-zwitterionic intermediate 14a. The barrier height for isomerization of 14a through the reverse reaction via TS-3 to 5a is very low. The highly asynchronous concerted transition state TS-4 connecting 5a and the *cis*-fused tricyclic product 15a is energetically more favorable than the rate-limiting second cyclization process of 14a (TS-5) for stepwise formation of the *trans*-fused tricyclic product 16a (see Figure 12). Thus, the *trans* intermediate 14a will not undergo the second cyclization process, but will

revert to **5a**, eventually funneling all of the material into the pathway leading to the *cis*-fused tricyclic product **15a** (Figures 10 and 12). Protonation of the anionic cyclopentadiene ring of **14a** may occur, but any protonation and deprotonation processes will be reversible regenerating **14a**, after which the reverse reaction can proceed to regenerate **5a**. Alternatively, base-mediated elimination may occur to convert the protonated intermediate directly to the starting material **5a** by the same mechanism as shown in Figure 9. Therefore, material taking nonproductive pathways will be recycled to **5a** leading to eventual exclusive conversion to the *cis*-fused tricyclic intermediates **15a** via the concerted transition state **TS-4**. This mechanism rationalizes the experimental observation that the *cis*-fused triquinane derivatives **4** are obtained exclusively.

Concerning the enamine, Seebach's group have shown that the *synclinal-exo* conformation (the dihedral angle of N–C–C–O) is the most stable in the solid state.³³ Although Shinisha and Sunoj calculated results for the Michael reaction of propanal and nitrostyrene catalyzed by diphenylprolinol silyl ether **1**,³⁹ they seem not to pay attention to this dihedral angle. Therefore, we performed a calculation of this enamine structure based on a *synclinal-exo* conformation. We optimized the structure of the model enamine prepared from propanal and diphenylprolinol silyl ether **1** shown in Figure 13 (see Figure 7, R = Me). We considered the *s-trans* conformation and *E* configuration for the enamine moiety (Figure 7).^{16i,33,39} For the C–C single bond at the 2-position, the *synclinal-exo* conformation (the dihedral angle of N–C–C–O) was assumed.³³ The B3LYP/6-311G(d,p)-optimized structure (Figure 13) indicates that the *gauche-syn* approach of the fulvene moiety to the *Re* face of the C–C double bond terminal of the enamine is effectively blocked by the diphenyltrimethylsilyloxymethyl group, and hence that *gauche-syn* attack of the fulvene moiety by the enamine double bond will exclusively take place from the less sterically hindered *Si* face of the enamine. We conclude that high enantioselectivities in the [6 + 2] cycloaddition reactions stem from the following two factors: (i) The enamine has a strong preference for the *s-trans* conformation and *E* configuration.^{16i,33,39} (ii) The bulky diphenyltrimethylsilyloxymethyl group at the 2-position of the pyrrolidine ring effectively differentiates the *Re*- and *Si*-faces of the enamine moiety for the *gauche-syn* mode approach of the enamine and fulvene moieties.

CONCLUSION

We have found that the diphenylprolinol silyl ether-mediated reaction of fulvenes having a δ -formylalkyl group at the exocyclic 6-position proceeds with excellent enantioselectivity to afford linear *cis*-fused triquinane derivatives. This is the first example of an organocatalyst-mediated, asymmetric, catalytic, intramolecular [6 + 2] cycloaddition. The formyl group in the substrates is initially converted into the corresponding enamine, after which an intramolecular cycloaddition occurs between the fulvene (6π) and the enamine (2π) functionalities. Computational investigations on model reaction sequences have shown that the model reaction of the intermolecular [6 + 2] cycloaddition proceeds in a stepwise mechanism via a zwitterionic intermediate. On the other hand, intramolecular [6 + 2] cycloaddition leading to the *cis*-fused linear triquinane skeleton proceeds in a concerted mechanism via a highly asynchronous transition state. C–C bond formation occurs through nucleophilic attack of the enamine double bond terminus at the exocyclic 6-position of the fulvene functionality,

while the second C–C bond is formed between the 1- or 4-position of the fulvene functionality and the nitrogen-neighboring carbon of the enamine moiety. The calculated structures indicate that the fulvene functionality approaches the enamine double bond in the *gauche-syn* conformation (Figure 5A). The energy profiles for the intramolecular reaction suggest that formation of the *trans*-zwitterionic intermediate is reversible. The experimental observation of exclusive formation of the *cis*-fused triquinane derivatives is rationalized as a consequence of reversible formation of the *trans*-zwitterionic intermediate and energetically favorable concerted formation of the *cis*-fused tricyclic product. The *s-trans* conformation and *E* configuration will be highly preferred in the enamine moiety, and quite effective enantiomeric differentiation of its π -faces in the *gauche-syn* mode of the C–C bond formation processes is achieved due to the bulkiness of the diphenyltrimethylsilyloxymethyl group on the pyrrolidine ring. These two factors are essential for high enantioselectivities in these [6 + 2] cycloaddition reactions.

ASSOCIATED CONTENT

S Supporting Information. Detailed experimental procedures, spectroscopic data of all new compounds. (i) Estimation procedure for the CCSD(T) level relation energy [$E_{\text{CCSD(T)}(\text{limit})}$] of each stationary point at the basis set limit, (ii) isomerization of the cycloaddition product **12**, (iii) Cartesian coordinates and absolute energies for all reported structures, (iv) energies of single-point calculations for the stationary points, (v) relative energies of the stationary points for the intramolecular [6 + 2] cycloaddition **5a**, (vi) MP2/6-311G(d,p) calculated energy profiles for the intramolecular cycloaddition **5a**, and (vii) the complete ref 18. This material is available free of charge via the Internet at <http://pubs.acs.org>.

AUTHOR INFORMATION

Corresponding Author

hayashi@ci.kagu.tus.ac.jp; t-uchimaru@aist.go.jp

ACKNOWLEDGMENT

I.K. is thankful to the Inoue Foundation for Science for a postdoctoral fellowship. This work was partially supported by a Grant-in-Aid for Scientific Research on Innovative Areas "Advanced Molecular Transformations by Organocatalysts" from The Ministry of Education, Culture, Sports, Science And Technology, Japan. Computations were performed on the AIST Super Cluster. We thank the Tsukuba Advanced Computing Center (TACC) in AIST for the provision of the computational facilities. We also thank the referees for their valuable comments and suggestions.

REFERENCES

- (1) For recent reviews: (a) *Comprehensive Asymmetric Catalysis*; Jacobsen, E. N., Pfaltz, A., Yamamoto, H., Eds.; Springer: New York, 1999. (b) *Cycloaddition Reaction in Organic Synthesis*; Kobayashi, S., Jørgensen, K. A., Eds.; Wiley-VCH: Weinheim, 2002.
- (2) For recent reviews of enantioselective Diels–Alder reactions: (a) Evans, D. A.; Johnson, J. S. In *Comprehensive Asymmetric Catalysis*; Jacobsen, E. N., Pfaltz, A., Yamamoto, H., Eds.; Springer: New York, 1999; Vol. 3, p 1177. (b) Corey, E. J. *Angew. Chem., Int. Ed.* **2002**, *41*, 1650. (c) Nicolaou, K. C.; Snyder, S. A.; Montagnon, T.; Vassilikogiannakis, G. *Angew. Chem., Int. Ed.* **2002**, *41*, 1668. (d) Hayashi, Y. *Catalytic*

Asymmetric Diels-Alder Reaction. In *Cycloaddition Reaction in Organic Synthesis*; Kobayashi, S., Jørgensen, K. A., Eds.; Wiley-VCH: Weinheim, 2002; pp 5–55.

(3) Woodward, R. B.; Hoffmann, R. *Angew. Chem., Int. Ed. Engl.* **1969**, *8*, 781.

(4) Fe complex: (a) Ward, J. S.; Pettit, R. *J. Am. Chem. Soc.* **1971**, *93*, 262. (b) Davis, R. E.; Dodds, T. A.; Hseu, T.-H.; Wagnon, J. C.; Devon, T.; Tancrede, J.; McKennis, J. S.; Pettit, R. *J. Am. Chem. Soc.* **1974**, *96*, 7562. Ti complex: (c) Mach, K.; Antropiusova, H.; Petrusova, L.; Hanus, V.; Turecek, F. *Tetrahedron* **1984**, *40*, 3295. (d) Kaagman, J. F.; Rep, M.; Horacek, M.; Sedmera, P.; Cejka, J.; Varga, V.; Mach, K. *Collect. Czech. Chem. Commun.* **1996**, *61*, 1722. Co complex: (e) Achard, M.; Tenaglia, A.; Buono, G. *Org. Lett.* **2005**, *7*, 2353. (f) Achard, M.; Mosrin, M.; Tenaglia, A.; Buono, G. *J. Org. Chem.* **2006**, *71*, 2907. Ru complex: (g) Itoh, K.; Mukai, K.; Nagashima, H.; Nishiyama, H. *Chem. Lett.* **1983**, 499. (h) Nagashima, H.; Matsuda, H.; Itoh, K. *J. Organomet. Chem.* **1983**, *258*, C15. (i) Ura, Y.; Utsumi, T.; Tsujita, H.; Wada, K.; Kondo, T.; Mitsudo, T. *Organometallics* **2006**, *25*, 2934. Mo complex: (j) Bourner, D. G.; Brammer, L.; Green, M.; Moran, G.; Orpen, A. G.; Reeve, C.; Schaverien, C. J. *J. Chem. Soc., Chem. Commun.* **1985**, 1409. (k) Schmidt, T. *Chem. Ber.* **1997**, *130*, 453. Cr complex: (l) Fischler, I.; Grevels, F. W.; Leitich, J.; Ozkar, J. *Chem. Ber.* **1991**, *124*, 2857. (m) Rigby, J. H.; Henshilwood, J. A. *J. Am. Chem. Soc.* **1991**, *113*, 5122. (n) Chaffee, K.; Sheridan, J. B.; Aistars, A. *Organometallics* **1992**, *11*, 18. (o) Rigby, J. H.; Sugathapala, P.; Heeg, M. J. *J. Am. Chem. Soc.* **1995**, *117*, 8851. (p) Rigby, J. H.; Warshakoon, N. C.; Heeg, M. J. *J. Am. Chem. Soc.* **1996**, *118*, 6094. (q) Chen, W.; Chaffee, K.; Chung, H. J.; Sheridan, J. B. *J. Am. Chem. Soc.* **1996**, *118*, 9980. (r) Kündig, E. P.; Robvieux, F.; Kondratenko, M. A. *Synthesis* **2002**, *14*, 2053 and references cited therein.

(5) Wender, P. A.; Correa, A. G.; Sato, Y.; Sun, R. *J. Am. Chem. Soc.* **2000**, *122*, 7815.

(6) Hong, B.-C.; Shr, Y.-J.; Wu, J.-L.; Gupta, A. K.; Lin, K.-J. *Org. Lett.* **2002**, *4*, 2249.

(7) Wu, T.-C.; Houk, K. N. *J. Am. Chem. Soc.* **1985**, *107*, 5308.

(8) Toselli, N.; Martin, D.; Achard, M.; Tenaglia, A.; Burgi, T.; Buono, G. *Adv. Synth. Catal.* **2008**, *350*, 280.

(9) Selected reviews on organocatalysis, see: (a) Dalko, P. I.; Moisan, L. *Angew. Chem., Int. Ed.* **2004**, *43*, 5138. (b) *Asymmetric Organocatalysis*; Berkessel, A., Groger, H., Eds.; Wiley-VCH: Weinheim, 2005. (c) Hayashi, Y. *J. Synth. Org. Chem. Jpn.* **2005**, *63*, 464. (d) List, B. *Chem. Commun.* **2006**, 819. (e) Marigo, M.; Jørgensen, K. A. *Chem. Commun.* **2006**, 2001. (f) Gaunt, M. J.; Johansson, C. C. C.; McNally, A.; Vo, N. T. *Drug Discovery Today* **2007**, *12*, 8. (g) *Enantioselective Organocatalysis*; Dalko, P. I., Ed.; Wiley-VCH: Weinheim, 2007. (h) Mukherjee, S.; Yang, J. W.; Hoffmann, S.; List, B. *Chem. Rev.* **2007**, *107*, 5471. (i) Walji, A. M.; MacMillan, D. W. C. *Synlett* **2007**, 1477. (j) MacMillan, D. W. C. *Nature* **2008**, *455*, 304. (k) Barbas, C. F., III. *Angew. Chem., Int. Ed.* **2008**, *47*, 42. (l) Dondoni, A.; Massi, A. *Angew. Chem., Int. Ed.* **2008**, *47*, 4638. (m) Melchiorre, P.; Marigo, M.; Carlone, A.; Bartoli, G. *Angew. Chem., Int. Ed.* **2008**, *47*, 6138. (n) Bertelsen, S.; Jørgensen, K. A. *Chem. Soc. Rev.* **2009**, *38*, 2178.

(10) For selected examples, see: (a) Ahrendt, K. A.; Borths, C. J.; MacMillan, D. W. C. *J. Am. Chem. Soc.* **2000**, *122*, 4243. (b) Northup, A. B.; MacMillan, D. W. C. *J. Am. Chem. Soc.* **2002**, *124*, 2458. (c) Wilson, R. M.; Jen, W. S.; MacMillan, D. W. C. *J. Am. Chem. Soc.* **2005**, *127*, 11616. (d) Ishihara, K.; Nakano, K. *J. Am. Chem. Soc.* **2005**, *127*, 10504. (e) Kim, K. H.; Lee, S.; Lee, D.-W.; Ko, D.-H.; Ha, D.-C. *Tetrahedron Lett.* **2005**, *46*, 5991. (f) Lemay, M.; Ogilvie, W. W. *Org. Lett.* **2005**, *7*, 4141. (g) Sakakura, A.; Suzuki, K.; Nakano, K.; Ishihara, K. *Org. Lett.* **2006**, *8*, 2229. (h) Kano, T.; Tanaka, Y.; Maruoka, K. *Org. Lett.* **2006**, *8*, 2687. (i) Sakakura, A.; Suzuki, K.; Ishihara, K. *Adv. Synth. Catal.* **2006**, *348*, 2457. (j) Lemay, M.; Ogilvie, W. W. *J. Org. Chem.* **2006**, *71*, 4663. (k) Lemay, M.; Aumand, L.; Ogilvie, W. W. *Adv. Synth. Catal.* **2007**, *349*, 441. (l) Kano, T.; Tanaka, Y.; Maruoka, K. *Chem. Asian J.* **2007**, *2*, 1161. (m) Gioia, C.; Hauville, A.; Bernardi, L.; Fini, F.; Ricci, A. *Angew. Chem., Int. Ed.* **2008**, *47*, 9236. (n) Ishihara, K.; Nakano, K.; Asakura, M. *Org. Lett.* **2008**, *10*, 2893. (o) Kano, T.; Tanaka, Y.; Osawa, K.; Yurino, T.; Maruoka, K. *Chem. Commun.* **2009**, 1956. Reviews, see:

(p) Lelais, G.; MacMillan, D. W. C. *Aldrichimica Acta* **2006**, *39*, 79.

(q) Erkkila, A.; Majander, I.; Pihko, P. M. *Chem. Rev.* **2007**, *107*, 5416.

(11) For selected examples, see: (a) Vicario, J. L.; Reboredo, S.; Badia, D.; Carrillo, L. *Angew. Chem., Int. Ed.* **2007**, *46*, 5168. (b) Guo, C.; Xue, M.-X.; Zhu, M.-K.; Gong, L.-Z. *Angew. Chem., Int. Ed.* **2008**, *47*, 3414.

(12) Ishihara, K.; Nakano, K. *J. Am. Chem. Soc.* **2007**, *129*, 8930.

(13) Harmata, M.; Ghosh, S. K.; Hong, X.; Wacharasindhu, S.; Kirchoefer, P. *J. Am. Chem. Soc.* **2003**, *125*, 2058.

(14) Selected examples: (a) Papageorgiou, C. D.; Cubillo de Dios, M. A.; Ley, S. V.; Gaunt, M. J. *Angew. Chem., Int. Ed.* **2004**, *43*, 4641. (b) Kunz, R. K.; MacMillan, D. W. C. *J. Am. Chem. Soc.* **2005**, *127*, 3240. (c) Johansson, C. C. C.; Bremeyer, N.; Ley, S. V.; Owen, D. R.; Smith, S. C.; Gaunt, M. J. *Angew. Chem., Int. Ed.* **2006**, *45*, 6024. (d) Hartikka, A.; Arvidsson, P. I. *J. Org. Chem.* **2007**, *72*, 5874. (e) Rios, R.; Sundén, H.; Vesely, J.; Zhao, G.-L.; Dziedzic, P.; Cordova, A. *Adv. Synth. Catal.* **2007**, *349*, 1028. (f) Xie, H.; Zu, L.; Li, H.; Wang, J.; Wang, W. *J. Am. Chem. Soc.* **2007**, *129*, 10886. (g) Lv, J.; Zhang, J.; Lin, Z.; Wang, Y. *Chem.-Eur. J.* **2009**, *15*, 972. (h) Terrasson, V.; Lee, A.; van der Figueiredo, R. M.; Campagne, J. M. *Chem.-Eur. J.* **2010**, *16*, 7875 and references cited therein.

(15) For reviews, see: (a) Palomo, C.; Mielgo, A. *Angew. Chem., Int. Ed.* **2006**, *45*, 7876. (b) Mielgo, A.; Palomo, C. *Chem. Asian J.* **2008**, *3*, 922.

(16) (a) Hayashi, Y.; Gotoh, H.; Hayashi, T.; Shoji, M. *Angew. Chem., Int. Ed.* **2005**, *44*, 4212. (b) Gotoh, H.; Masui, R.; Ogino, H.; Shoji, M.; Hayashi, Y. *Angew. Chem., Int. Ed.* **2006**, *45*, 6853. (c) Gotoh, H.; Hayashi, Y. *Org. Lett.* **2007**, *9*, 2859. (d) Hayashi, Y.; Okano, T.; Aratake, S.; Hazeldard, D. *Angew. Chem., Int. Ed.* **2007**, *46*, 4922. (e) Gotoh, H.; Ishikawa, H.; Hayashi, Y. *Org. Lett.* **2007**, *9*, 5307. (f) Hayashi, Y.; Gotoh, H.; Masui, R.; Ishikawa, H. *Angew. Chem., Int. Ed.* **2008**, *47*, 4012. (g) Hayashi, Y.; Itoh, T.; Ohkubo, M.; Ishikawa, H. *Angew. Chem., Int. Ed.* **2008**, *47*, 4722. (h) Hayashi, Y.; Samanta, S.; Gotoh, H.; Ishikawa, H. *Angew. Chem., Int. Ed.* **2008**, *47*, 6634. (i) Hayashi, Y.; Okano, T.; Itoh, T.; Urushima, T.; Ishikawa, H.; Uchimaru, T. *Angew. Chem., Int. Ed.* **2008**, *47*, 9053. (j) Hayashi, Y.; Toyoshima, M.; Gotoh, H.; Ishikawa, H. *Org. Lett.* **2009**, *11*, 45. (k) Hayashi, Y.; Obi, K.; Ohta, Y.; Okamura, D.; Ishikawa, H. *Chem. Asian J.* **2009**, *4*, 246. (l) Gotoh, H.; Hayashi, Y. *Chem. Commun.* **2009**, 3083. (m) Gotoh, H.; Okamura, D.; Ishikawa, H.; Hayashi, Y. *Org. Lett.* **2009**, *11*, 4056.

(17) (a) Marigo, M.; Wabnitz, T. C.; Fielenbach, D.; Jørgensen, K. A. *Angew. Chem., Int. Ed.* **2005**, *44*, 794. (b) Marigo, M.; Fielenbach, D.; Braunton, A.; Kjasgaard, A.; Jørgensen, K. A. *Angew. Chem., Int. Ed.* **2005**, *44*, 3703. For recent reports, see: (c) Nielsen, M.; Borch, J. C.; Paixao, M. W.; Holub, N.; Jørgensen, K. A. *J. Am. Chem. Soc.* **2009**, *131*, 10581.

(18) Frisch, M. J.; et al. *Gaussian 03*, revision D.01; Gaussian, Inc.: Wallingford, CT, 2004.

(19) (a) Becke, A. D. *J. Chem. Phys.* **1993**, *98*, 1372. (b) Becke, A. D. *J. Chem. Phys.* **1993**, *98*, 5648. (c) Lee, C.; Yang, W.; Parr, R. G. *Phys. Rev. B* **1988**, *37*, 785.

(20) (a) Møller, C.; Plesset, M. S. *Phys. Rev.* **1934**, *46*, 618. (b) Head-Gordon, M.; Pople, J. A.; Frisch, M. J. *Chem. Phys. Lett.* **1988**, *153*, 503.

(21) Krishnan, R.; Binkley, J. S.; Seeger, R.; Pople, J. A. *J. Chem. Phys.* **1980**, *72*, 650.

(22) (a) Gonzalez, C.; Schlegel, H. B. *J. Chem. Phys.* **1989**, *90*, 2154. (b) Gonzalez, C.; Schlegel, H. B. *J. Phys. Chem.* **1990**, *94*, 5523.

(23) Pople, J. A.; Head-Gordon, M.; Raghavachari, K. *J. Chem. Phys.* **1987**, *87*, 5968.

(24) The details of the procedure for estimating the $E_{\text{CCSD(T)}(\text{limit})}$ are given in the Supporting Information. The relative energies calculated for the B3LYP- and MP2-optimized stationary-point structures did not differ significantly: the differences were less than 1.5 kcal/mol. We calculated relative enthalpy values for the MP2-optimized stationary points by using the $E_{\text{CCSD(T)}(\text{limit})}$ relative energies and the enthalpy correction terms derived from the MP2 calculations. For zero-point energy corrections, the MP2/6-311G(d,p) frequencies were scaled by a factor of 0.9663.^{25a} For enthalpy and entropy (at 298.15 K) calculations, the recommended scaling factors for the MP2/6-311G(d,p) frequencies are 1.0061 and 1.0175, respectively.^{25b} These factors are close to 1.0, and

thus the MP2 enthalpy and entropy correction terms derived from the harmonic approximation were used without scaling.

(25) (a) Irikura, K. K.; Johnson, R. D., III; Kacker, R. N.; Kessel, R. *J. Chem. Phys.* **2009**, *130*, 114102. (b) Scott, A. P.; Radom, L. *J. Phys. Chem.* **1996**, *100*, 16502.

(26) (a) Barone, V.; Cossi, M. *J. Phys. Chem. A* **1998**, *102*, 1995. (b) Cossi, M.; Rega, N.; Scalmani, G.; Barone, V. *J. Comput. Chem.* **2003**, *24*, 669.

(27) Takano, Y.; Houk, K. N. *J. Chem. Theory Comput.* **2005**, *1*, 70.

(28) The atomic polar tensor-based charges (Cioslowski, J. *J. Am. Chem. Soc.* **1989**, *111*, 8333) indicate that the total charges of NMe₂ and cyclopentadiene moieties of MP2/6-311G(d,p)-optimized **11** are +0.7072 and -0.8773, respectively.

(29) The intermediate **11**, as well as the transition states **TS-1** and **TS-2**, was a pure singlet closed-shell species with $S^2 = 0$. We also considered the possibility of a radical-pair-like intermediate for the stepwise C–C bond formation process. We tried to locate such an open-shell intermediate by using the unrestricted method, but this did not locate any diradical species along the [6 + 2] reaction coordinate.

(30) The dihedral angle of C5–C6–C2'–C1' is -62.80° in the B3LYP energy minimum of the zwitterionic intermediate **11** (see Table 3). In the B3LYP calculation, separation of the intermediate **11** into the reactants fulvene **7** and enamine **8** occurred in the C5–C6–C2'–C1' dihedral angle region from -100° to -105°. Meanwhile, the spontaneous conversion of **11** into the cycloaddition product **12** was observed in the C5–C6–C2'–C1' dihedral angle region of -5° to -10°. The zwitterionic state will therefore be maintained within the C5–C6–C2'–C1' dihedral angle region from -10° to -100°. Except for within this dihedral angle region, the zwitterionic structure will collapse. Geometry optimization starting from the *gauche-anti* (B) conformation resulted in separation into fulvene **7** and enamine **8**. These results imply that the *gauche-syn* conformation is electrostatically stabilized. If the positively charged NMe₂ moiety and the negatively charged cyclopentadiene ring are forced to be located distantly, the charge separated electronic structure will be energetically unfavorable, and the zwitterionic structure collapses.

(31) The dimethylamino group in the *trans* isomer of the cycloaddition product **12** is positioned on the inner face of the two five-membered rings (Figure 4). This *trans* isomer was found to be less stable by 1.80 kcal/mol than the *cis* isomer having the dimethylamino group on the outer side of the two rings. In pursuit of a pathway leading to the *cis* isomer of the product, the potential energy surface was explored. Neither a reaction pathway connecting the zwitterionic intermediate **11** and the *cis* product nor a [6 + 2] cycloaddition pathway directly leading to the *cis* product was found. Instead, a pathway for isomerization between the *trans* cycloaddition product **12** and its *cis* isomer was located. (See the Supporting Information.)

(32) The CPCM calculations suggested a pronounced solvation effect for the zwitterionic intermediate **11** and **TS-2** (Table 4). For these stationary points, the solution-phase relative enthalpy values are calculated to be lower than the corresponding gas-phase values by about 5 kcal/mol. For the final products **9** and **10**, the solution-phase relative enthalpy is about 0.6 kcal/mol lower than the gas-phase value. Meanwhile, the solvation effects are found to be relatively small for **TS-1** and the cycloaddition product **12**. The differences between the gas-phase and solution-phase relative enthalpy values for **TS-1** and **12** are less than 0.5 kcal/mol.

(33) (a) Seebach, D.; Groselj, U.; Badine, D. M.; Schweizer, W. B.; Beck, A. K. *Helv. Chim. Acta* **2008**, *91*, 1999. (b) Groselj, U.; Seebach, D.; Badine, D. M.; Schweizer, W. B.; Beck, A. K.; Krossing, I.; Klose, P.; Hayashi, Y.; Uchimaru, T. *Helv. Chim. Acta* **2009**, *92*, 1225.

(34) A scaling factor of 0.9877 was used for the B3LYP/6-311G(d,p) frequencies. Andersson, M. P.; Uvdal, P. *J. Phys. Chem. A* **2005**, *109*, 2937. See ref 25a for the scaling factor of the MP2/6-311G(d,p) frequencies.

(35) The calculated energy differences between the *cis* and *trans* isomers **13a** and **14a** were 2.52 and 1.24 kcal/mol (including the zero-point energies³⁴) at the B3LYP/6-311G(d,p) and MP2/6-311G(d,p)

levels, respectively. The optimized structures of the *cis* and the *trans* isomers **13a** and **14a** take the *gauche-syn* conformation. The B3LYP-optimized dihedral angles (corresponding to the C5–C6–C2'–C1' dihedral angle in the model) were -51.2° and -69.2° for **13a** and **14a**, respectively, while the MP2-optimized dihedral angles were -52.0° and -66.1°.

(36) The C–C bond distance between the 6-position of the fulvene moiety and the C–C double bond terminal of the enamine moiety (C6–C2') in **TS-4** is, respectively, 1.7200 and 1.8180 Å in B3LYP- and MP2-optimized structures (Table 5). These bond distances are slightly longer than the corresponding bond lengths in the *cis*-fused tricyclic product **15a** (Table 5, 1.5822 and 1.5731 Å). Meanwhile, the other forming bond in **TS-4** (C1–C1'), the C–C bond between the 1-position of the fulvene moiety and the carbon atom adjacent to the nitrogen of the enamine moiety, is quite long, more than 3 Å, 3.0939 and 3.1557 Å in B3LYP and MP2 structures (Table 5). These bond lengths are much longer than the corresponding B3LYP and MP2 C–C bond distances of 1.5751 and 1.5404 Å in **15a**, and are also considerably longer than the B3LYP and MP2 bond distances, 2.8310 and 2.4960 Å in **TS-5** (Table 5).

(37) The numerical values and the MP2 energy profiles are given in the Supporting Information.

(38) After considering solvation energy, **TS-4** is still energetically favorable over **TS-5**. CPCM calculations suggested solvation energies of 5.78 and 6.66 kcal/mol for the B3LYP geometries of **TS-4** and **TS-5**. The corresponding values for the MP2 geometries were 4.53 and 4.51 kcal/mol. As a consequence, the B3LYP and MP2 geometries suggest that **TS-4** will be lower by 1.70 and 3.87 kcal/mol than **TS-5** in toluene solution.

(39) Shinisha, C. B.; Sunoj, R. B. *Org. Biomol. Chem.* **2008**, *6*, 3921.